

Post-Asymptotic Giant Branch Evolution of Low- and Intermediate-Mass Stars. Preliminary Results.

Marcelo M. Miller Bertolami^{1,2,†}

¹*Max-Planck-Institut für Astrophysik, Karl-Schwarzschild-Str. 1, 85748, Garching, Germany; marcelo@MPA-Garching.MPG.DE*

²*Instituto de Astrofísica de La Plata, UNLP-CONICET, Paseo del Bosque s/n, 1900 La Plata, Argentina; mmiller@fcaglp.unlp.edu.ar*

[†]*Postdoctoral fellow of the Alexander von Humboldt Foundation*

Abstract. Preliminary results from an ongoing project to compute a grid of post-AGB models is presented. Our preliminary results show that stellar evolution computations that include an updated treatment of the microphysics predict post-AGB timescales that are several times shorter than predicted by older models. Also the mass-luminosity relation of post-AGB models deviates from that of older grids. In addition, our results suggest only a slight metallicity dependence of the post-AGB timescales. We expect these results to have significant consequences for models of the formation of planetary nebulae and their luminosity function.

1. Introduction

Planetary Nebulae (PNe) are among the most beautiful astronomical objects. They are the result of the evolution of low- and intermediate-mass stars ($M_{\text{ZAMS}} \sim 0.8\text{--}8 M_{\odot}$). In the most simple scenario, PNe are formed when the progenitor stars lose their external envelopes at the end of the Asymptotic Giant Branch (AGB) and cross the HR-diagram on their way to the white dwarf cooling sequence. While crossing the HR-diagram the central stars of the PNe (CSPNe) become sufficiently hot to ionize the previously ejected material (Shklovsky 1957; Abell & Goldreich 1966; Paczyński 1970).

Besides being interesting and fascinating objects in themselves their properties are also useful for other fields of astrophysics (Kwitter et al. 2014). PNe and CSPNe offer unique insight into the nucleosynthesis during previous evolutionary phases like the AGB. Extragalactic PNe can be used to understand metallicity gradients and their temporal evolution in galaxies. Also, the PNe luminosity function (PNLF) has proven to be a good distance indicator as far as $\sim 20\text{Mpc}$, but we still do not understand why (Ciardullo 2012). The formation and detectability of PNe depends strongly on the relationship between two different timescales. The evolutionary timescale of the CSPNe, which provides the ionizing photons, and the dynamical timescales of the circumstellar material ejected at the end of the AGB. If the CSPN evolves too fast the PN will be ionized for a short time, and thus will have a low detection probability, or might even not be ionized at all. On the other hand, if the star evolves too slowly, the ionization of the nebula will take place when the ejected material has already dispersed too much

to be detectable. In this work we address the first of these timescales. Namely, we present preliminary results from full stellar evolution computations of the post-AGB and CSPNe phases that include an updated treatment of macro and microphysics. This stage is one of the least understood phases of low- and intermediate mass stars and there are some indications that current models are not accurate enough, e.g. a) The two available grids of post-AGB models (Vassiliadis & Wood 1994; Bloeker 1995) do not agree on the predicted timescales (Zijlstra et al. 2008), b) The CSPNe mass-luminosity relation seems to be at variance with the constraints coming from hydrodynamically consistent model atmospheres (Pauldrach et al. 2004), c) consistency between the masses of white dwarfs and those of CSPNe determined by asteroseismology requires faster evolutionary speeds (Gesicki et al. 2014). In addition, until now we do not understand why the cut-off of the PNe luminosity function is constant in most galaxies. Last, but not least, Marigo (2002) showed that C-rich molecular opacities are key to predict the right effective temperatures once the AGB models become carbon rich ($C/O > 1$, by number fraction). These inconsistencies and the fact that available post-AGB models are based on very old radiative opacities and microphysics calls for a restudy of the problem.

2. Physical details of the stellar evolution models

The computations presented in this work have been performed with LPCODE stellar evolution code. A detailed description of the code can be found in Althaus et al. (2013), and references therein, here focus on the physical ingredients, and updates, which are particularly relevant for the present work. In the pre-WD regime LPCODE uses the OPAL EOS_2005 equation of state for H- and He rich mixtures and a simplified EOS for other compositions. Updated high- and low- temperature radiative opacities are included according to Iglesias & Rogers (1996) and Ferguson et al. (2005). This includes pretabulated C-rich molecular opacities (Weiss & Ferguson 2009). The $^{14}\text{N}(p,\gamma)^{15}\text{O}$ reaction rate, that sets the overall efficiency of the CNO-cycle, was taken from Imbriani et al. (2005). Convective mixing is treated within mixing length theory (MLT) and a diffusive convective picture, including an exponentially decaying velocity field outside formal convective boundaries (with a free parameter f , see Herwig et al. 1997 for details). From the calibration of the solar model with diffusion we obtain $\alpha_{\text{MLT}} = 1.825$. The value of f in convective cores is set to $f = 0.0174$ from the calibration of the width of the upper main sequence. This equivalent to an overshooting extension of 0.2 times the pressure scale height. The values of f in the pulse driven convection zone (PDCZ) during the thermal pulses in the AGB is set to $f^{\text{PDCZ}} = 0.005$ which allows to reproduce the range of He, C and O ratios observed in PG1159 type stars (Werner & Herwig 2006). The f -value at the bottom of the convective envelope is taken to be $f^{\text{CE}} = 0.1$ (Herwig 2005). Winds are a decisive aspect of AGB evolution since they determine when the TP-AGB phase ends. To include the impact of the transition from an O-rich AGB to a C-rich AGB star we implemented different wind prescriptions for the O- and C-rich dust driven winds. For the sake of consistency we choose dust driven wind prescriptions derived by the same authors and methods, ($\log \dot{M} = 4.08 \log P - 16.54$ Groenewegen et al. 1998 and $\log \dot{M} = -9 + 0.0032 P$ Groenewegen et al. 2009; where P is the pulsation period). For the pre-dusty winds we included the Schröder & Cuntz (2005) which seems to reproduce some RGB and AGB observables better than the standard Reimers prescription (Girardi et al. 2010). Finally, for the hot radiative driven winds we adopted

a mass loss prescription, $\dot{M} = 9.8 \times 10^{-15} \times (L/L_{\odot})^{1.674}$, which is based on the results of Pauldrach et al. (2004) and similar to the one adopted by Bloeker (1995). Between the hot and cold wind regime, $3.8 \lesssim \log T_{\text{eff}} \lesssim 4.1$, there are no available prescriptions and we had to rely on interpolations.

3. Preliminary results and discussion

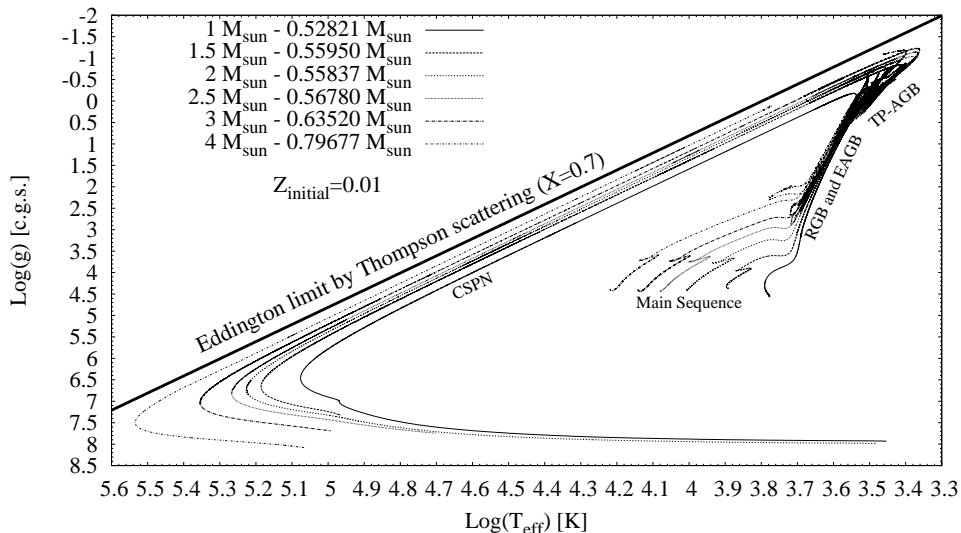


Figure 1. $\log T_{\text{eff}} - \log g$ -diagram of the computed sequences for $Z=0.01$.

It is well known that the computation of the very end of the TP-AGB is riddled with convergence problems (Weiss & Ferguson 2009; Lau et al. 2012). This implies that a lot of human time (baby-sitting) is required to compute the transition from the TP-AGB to the CSPNe phase. Even when codes converge, convergence happens at the expense of a prohibitively small timesteps (even down to $\Delta t \sim 1$ hour). Despite all numerical improvements our computations are not the exception. Consequently, the number of complete simulations presented in this work is rather small. In Fig. 1 we show the $\log T_{\text{eff}} - \log g$ -diagram (“Kiel diagram”) for our $Z = 0.01$ sequences. Table 1 shows the most relevant quantities of our TP-AGB and post-AGB stellar models. A comparison of the M_i - M_f relationship of our models (Table 1) with semiempirical determinations from stellar clusters (Salaris et al. 2009), common proper motion pairs (Catalán et al. 2008) or the Galactic bulge (Gesicki et al. 2014) suggest that our values of M_f may be somewhat low. This is very likely the consequence of too strong third dredge up during the TP-AGB (Salaris et al. 2009). In fact, this causes the formation of C-rich stars already at the first thermal pulse in our low metallicity sequences ($Z=0.001$ and $M_i = 1.5$ and $2.5 M_{\odot}$). This might lead to disagreements with the carbon star luminosity function and thus to a need to re-calibrate the overshooting parameters during the TP-AGB. However, it should be notice that the value of $f^{\text{PDCZ}} \sim 0.005$ is required to reproduce the abundances of PG1159 type post-AGB stars, leaving only f^{CE} as a possible free parameter.

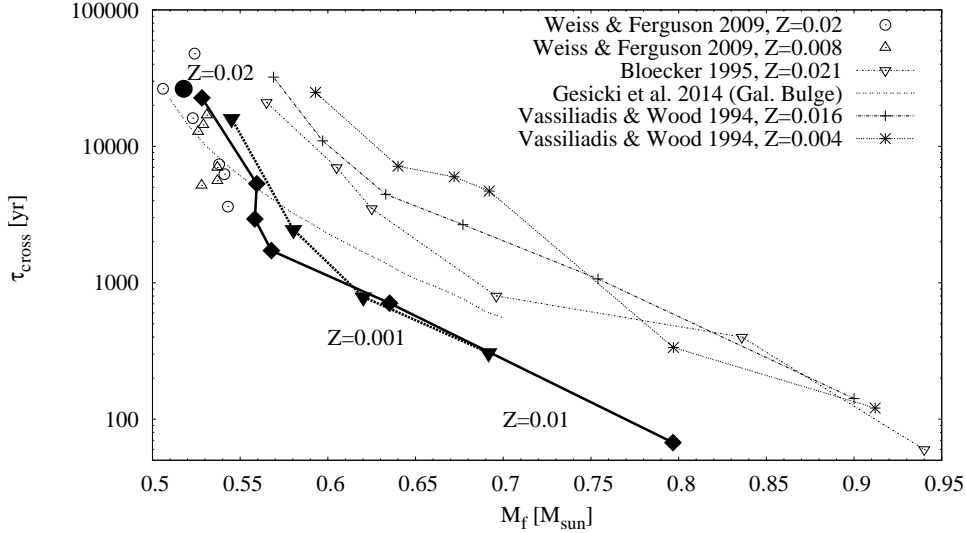


Figure 2. Crossing times (τ_{cross}) from different sources as compared with our results for H-burning post-AGB sequences. Filled symbols indicate the predicted crossing times for $Z=0.02$, 0.01 , 0.001 ; circles, rhombi and triangles respectively.

A comparison of our timescales with those of previous models and semiempirical determinations (see Fig. 2) allow us for some very interesting preliminary conclusions. On one hand, in the range of remnant masses where our models overlap with those of Weiss & Ferguson (2009) the agreement is quite good. This is particularly interesting in the light of the different numerical codes and wind prescriptions adopted. This suggests that the details of mass loss might not play a crucial role in the determination of post-AGB timescales. Given the uncertainties behind this ingredient of stellar evolution computations, this might be a good news. On the other hand, our models predict much shorter (up to a factor of ~ 5 !) post-AGB timescales than those of Vassiliadis & Wood (1994) and Bloeker (1995). In the light of the agreement between our timescales and those of Weiss & Ferguson (2009) this suggests that stellar evolution computations based on old microphysics might have significantly overestimated the length of the CSPNe phase. Interestingly enough our much shorter timescales are in agreement with the results from studies of PNe (Gesicki & Zijlstra 2007; Gesicki et al. 2014) that suggests that CSPNe should evolve several times faster than predicted by old stellar evolution models. Last, but not least, our models do not predict a strong dependence of the post-AGB timescales with metallicity. In addition, the post-AGB mass-luminosity relation of modern models is different from that of old grids. All these results, if confirmed, will have an impact in the predictions of models for the formations of PNe in different stellar populations. In particular, the impact of modern post-AGB computations in the formation of the PNLf needs to be assessed.

References

- Abell, G. O., & Goldreich, P. 1966, *PASP*, 78, 232
 Althaus, L. G., Miller Bertolami, M. M., & Córscico, A. H. 2013, *A&A*, 557, A19.

Table 1. Properties of the AGB and post-AGB (H-burning) stellar evolution models: metallicity (Z), initial mass (M_i), final mass (M_f), number of thermal pulses on the AGB (N_{TP}), age of the model at the first thermal pulse (τ_{1TP}), length of the O-rich TP-AGB (τ_O), length of the C-rich TP-AGB (τ_C), the luminosity of the post-AGB remnant in the plateau phase ($L_{\log T_{\text{eff}}=4}^{\text{post-AGB}}$, taken at $\log T_{\text{eff}} = 4$), and the crossing time (τ_{cross}) of the post-AGB remnant from $\log T_{\text{eff}} = 4$ to the point of maximum effective temperature (“knee”, see Fig. 1).

Z	M_i [M_{\odot}]	M_f [M_{\odot}]	N_{TP}	τ_{1TP} [Myr]	τ_O [Kyr]	τ_C [Kyr]	$L_{\log T_{\text{eff}}=4}^{\text{post-AGB}}$ [L_{\odot}]	τ_{cross} [yr]
0.02	1.0	0.51781	3	11923	626 \lesssim	0	2966	26407
0.01	1.0	0.52821	4	10510	728 \lesssim	0	3396	22660
0.01	1.5	0.55950	7	2584	814	260 \lesssim	5674	5319
0.01	2.0	0.55837	12	1206	1513	654 \lesssim	6624	2936
0.01	2.5	0.56780	11	720	611	1105 \lesssim	7700	1722
0.01	3.0	0.63520	8	431	177	345 \lesssim	10524	708
0.01	4.0	0.79677	11	195	28	109 \lesssim	18270	~ 67
0.001	1.0	0.54510	4	6594	625	249 \lesssim	4477	15983
0.001	1.5	0.58039	7	1754	0	1017 \lesssim	8100	2454
0.001	2.0	0.62018	10	797	82	774 \lesssim	11434	787
0.001	2.5	0.69163	12	492	0	570 \lesssim	14920	307

- Bloecker, T. 1995, *A&A*, 299, 755
Catalán, S., Isern, J., García-Berro, E., Ribas, I., Allende Prieto, C., & Bonanos, A. Z. 2008, *A&A*, 477, 213.
Ciardullo, R. 2012, *Ap&SS*, 341, 151.
Ferguson, J. W., Alexander, D. R., Allard, F., Barman, T., Bodnarik, J. G., Hauschildt, P. H., Heffner-Wong, A., & Tamanai, A. 2005, *ApJ*, 623, 585.
Gesicki, K., & Zijlstra, A. A. 2007, *A&A*, 467, L29.
Gesicki, K., Zijlstra, A. A., Hajduk, M., & Szyszka, C. 2014, *A&A*, 566, A48.
Girardi, L., Williams, B. F., Gilbert, K. M., et al. 2010, *ApJ*, 724, 1030.
Groenewegen, M. A. T., Sloan, G. C., Soszyński, I., & Petersen, E. A. 2009, *A&A*, 506, 1277.
Groenewegen, M. A. T., Whitelock, P., Smith, C., & Kerschbaum, F. 1998, *MNRAS*, 293, 18
Herwig, F. 2005, *ARA&A*, 43, 435
Herwig, F., Bloecker, T., Schoenberner, D., & El Eid, M. 1997, *A&A*, 324, L81.
Iglesias, C. A., & Rogers, F. J. 1996, *ApJ*, 464, 943
Imbriani, G., Costantini, H., Formicola, A., et al. 2005, *European Physical Journal A*, 25, 455.
Kwitter, K. B., Méndez, R. H., Peña, M., et al. 2014, *ArXiv e-prints*. 1403.2246
Lau, H. H. B., Gil-Pons, P., Doherty, C., & Lattanzio, J. 2012, *A&A*, 542, A1.
Marigo, P. 2002, *A&A*, 387, 507.
Paczynski, B. 1970, *Acta Astron.*, 20, 47
Pauldrach, A. W. A., Hoffmann, T. L., & Méndez, R. H. 2004, *A&A*, 419, 1111.
Salaris, M., Serenelli, A., Weiss, A., & Miller Bertolami, M. 2009, *ApJ*, 692, 1013.
Schröder, K.-P., & Cuntz, M. 2005, *ApJ*, 630, L73.
Shklovsky, I. S. 1957, in *Non-stable stars*, ed. by G. H. Herbig, vol. 3 of *IAU Symposium*, 83
Vassiliadis, E., & Wood, P. R. 1994, *ApJS*, 92, 125
Weiss, A., & Ferguson, J. W. 2009, *A&A*, 508, 1343.
Werner, K., & Herwig, F. 2006, *PASP*, 118, 183.
Zijlstra, A. A., van Hoof, P. A. M., & Perley, R. A. 2008, *ApJ*, 681, 1296.